Nuclear Instruments and Methods in Physics Research A 340 (1994) 304–308
North-Holland

NUCLEAR INSTRUMENTS & METHODS IN PHYSICS RESEARCH
Section A

The H1 forward muon spectrometer

H. Cronström [a], V. Hedberg [a], C. Jacobsson [a], L. Jönsson [a,*], H. Lohmander [a], M. Nyberg [a], I. Kenyon [b], H. Phillips [b], P. Biddulph [c], P. Finnegan [c], J. Foster [c], S. Gilbert [c], C. Hilton [c], M. Ibbotson [c], A. Mehta [c], P. Sutton [c], K. Stephens [c], R. Thompson [c]

[a] *Physics Department, University of Lund, Lund, Sweden*
[b] *School of Physics and Space Research, University of Birmingham, Birmingham, UK*
[c] *Physics Department, University of Manchester, Manchester, UK*

Received 21 September 1993

The H1 detector started taking data at the electron–proton collider HERA in the beginning of 1992. In HERA 30 GeV electrons collide with 820 GeV protons giving a strong boost of the centre-of-mass system in the direction of the proton, also called the forward region. For the detection of high momentum muons in this region a muon spectrometer has been constructed, consisting of six drift chamber planes, three either side of a toroidal magnet. A first brief description of the system and its main parameters as well as the principles for track reconstruction and T_0 determination is given.

1. General description

The purpose of the forward muon spectrometer is to measure high energy muons in the range of polar angles $3° \leqslant \theta \leqslant 17°$. The detector consists of drift chamber planes, either side of a toroidal magnet. The design specifications aim at measuring the momenta of muons in the range between 5 and 200 GeV/c, the lower limit being given by the amount of material the muons have to penetrate and the influence on the momentum resolution of the multiple Coulomb scattering in the magnet iron. The upper limit is set by the magnetic field strength of the toroid together with the spatial resolution of the drift chambers. The expected momentum resolution at 5 GeV/c is 24% and deteriorates slowly to 36% at 200 GeV/c above which there is a danger of misidentifying the charge of the muon. Muon momenta below 5 GeV/c will be measured in the forward tracker.

Fig. 1a shows schematically the detector arrangement and the toroid magnet. The drift chamber planes, which increase in size from about 4 m diameter for the first detector plane to 6 m diameter for the last, are all divided into octants which are formed from individual drift cells accurately mounted on Al-frames. The orientation of the drift cells is such that four of the planes essentially measure the polar angle (θ) and thereby provide the momentum of the traversing muon whilst the remaining two measure the azimuthal angle (ϕ). Each plane consists of a double layer of drift cells such that each layer is displaced with respect to the other by half a cell width (Fig. 1b). This arrangement enables the resolution of left–right ambiguities and also the determination of T_0 as will be explained below. The total number of drift cells is 1520.

The toroid is 1.2 m thick and constructed out of eight semicircular steel modules with an inner radius of 0.65 m and an outer radius of 2.9 m. Each of the twelve rectangular coils which provide the field consists of 15 turns of watercooled Cu-tube, 11.5×11.5 mm^2. At a current of 150 A the field strength varies from about 1.75 T at the inner radius to about 1.5 T at the outer radius. Field measurements made in the centre of each coil show a variation of less than 1%. A more detailed description of the toroid magnet can be found in ref. [1].

2. Chamber design

All drift cells have a rectangular cross section with a depth of 2 cm, a width of 12 cm and lengths between 40 and 240 cm. With a central sense wire the maximum drift distance becomes 6 cm. The cells have 50 μm thick nichrome wires except for the inner short cells where the diameter is 40 μm. For cells longer than 1.5 m there is a wire support in the middle. As illustrated in Fig. 2 each cell comprises two PCB planes, copper-coated on both sides, and 0.7 mm thin extruded Al-

* Corresponding author

SSDI 0168-9002(93)E1039-Z

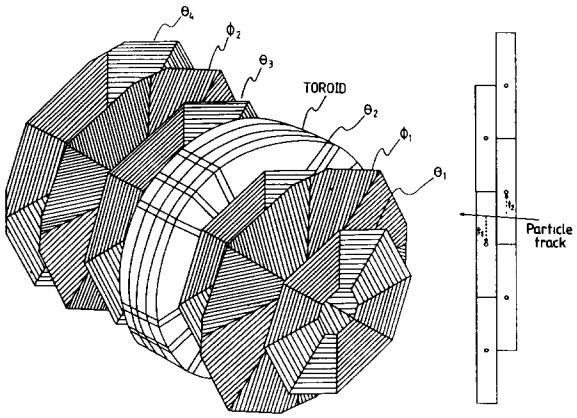

Fig. 1. (a) A schematic view of the forward muon spectrometer and (b) the cell structure of a double layer.

profiles to minimise the dead space between cells. The outer copper surface of the PCB is kept at ground to form a screened box while the inner surface has been machined to give 4 mm wide strips. These are used as drift electrodes connected to a 230 MΩ metal film resistor chain mounted on the end cap to obtain a uniform drift field. The end caps are made of moulded Noryl with high precision holes to locate the crimp pins for fixing the sense wires and provide holes for the gas connections. One end contains the high voltage distribution resistor chain and the sense wire readout connection isolated via a 1 nF ceramic disc capacitor. Sense wires of adjacent cells are linked together via a 330 Ω resistor at the other end forming the equivalent of a U-shaped cell which then is read out at both ends. This allows not only a determination of the track position transverse to the sense wire from the measurement of the drift time but also the coordinate along the wire by charge division measurement and thereby giving information on which cell of a coupled pair was hit.

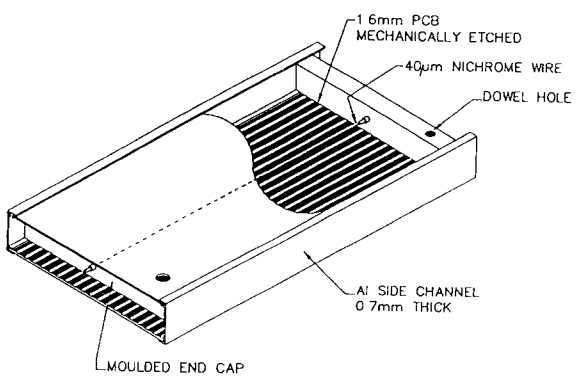

Fig. 2. The construction of a drift cell.

3. The chamber gas and high voltage system

The choice of gas for the drift chambers was determined by several requirements. One is the desire to work in a drift voltage range where the drift velocity is constant. Further the gas has to be fast enough for the pulse to arrive in time for the trigger and finally it should be nonflammable for safety reasons. Currently the so-called FMS gas (forward muon spectrometer gas), which is a mixture of 92.5% argon, 5% CO_2 and 2.5% methane, has been chosen for the chambers. The gas is mixed and purified in a recirculator [2]. The chambers have a total gas volume of 4 m^3, and with a small overpressure of about 0.2 mbar measured at the output, the return gas flow is typically 90% of the input and the oxygen content is measured to be of order 100 ppm. For the FMS gas the drift velocity as a function of the drift field voltage, corrected for atmospheric pressure, is shown in Fig. 3. An average drift field of 480 V/cm gives the desired drift velocity of ~ 5 cm/μs. The drift field is defined by an increasing positive potential from the cathode at ground to +2.88 kV on the centre electrode at the position of the sense wire. The sense wire is kept typically at 4.21 kV for the 40 μm wires and at 4.26 kV for the 50 μm wires. The gas gain is controlled by the difference in voltage between the sense wire and the drift field close to the wire.

A 120-channel CAEN 127 system supplies distribution boxes on the detector with high voltage via 50 m long coaxial cables. One 6 kV 1 mA module supplies drift voltage to an entire octant, feeding 20–40 individual resistor chains. Similarly an 8 kV 200 μA module supplies the sense voltage to all but the 12 innermost cells of a θ-octant, which in case of bad beam conditions might be set to a lower voltage. For the φ-octants the central section which is close to the beam tube can be moved outwards mechanically by remote controls and thus there is no need for any special HV arrangement.

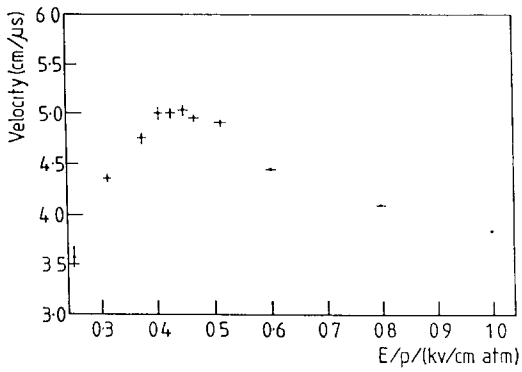

Fig. 3. The drift velocity versus the drift voltage, corrected for atmospheric pressure, for the FMS gas.

There is a continuous monitoring of the gas composition and flow rates as well as of the high voltage, communicated via an Apple Macintosh II ci in the control room. From this work station it is also possible to control the high voltage of the detector and the toroid magnet.

4. The readout system

The signals are read out into 8 channel preamplifiers of standard H1 design [3] mounted close to the cells. The output pulses are driven down 50 m long coaxial cables to F1001 flash analogue to digital converters (FADC) [3] run in common stop mode. Signals are digitised with the equivalent of 10 bit resolution (8 bit nonlinear response) in 9.6 ns time bins, phase locked to the HERA beam crossing frequency. These are stored in a circular buffer with a depth of 256 time bins. Each crate of 256 FADCs is controlled by a scanner [4] which on receiving the first trigger stops the buffer and scans the preceding 256 digitisings for hits. Each scanner then transfers the zero suppressed data to a front end processor where the pulses are analysed to extract start times and charge contents.

5. The charge–time analysis

Only the rising edge and peak region of a pulse is used to get the time and charge information. A pulse is said to start when there are two successively rising digitisings above threshold. The end of a pulse is taken as the second successive digitising after the peak which is below threshold, or eight 9.6 ns time bins from the start of the pulse, whichever occurs first. The arrival time of the pulse is obtained by extrapolating a line fitted to the steepest part of the leading edge back to the intercept with the background level. With a test setup, looking at cosmic muons, this method gave a resolution of < 200 μm as illustrated in Fig. 4. This result was obtained with a gas mixture of 90% argon and 10% propane providing a drift velocity of 4 cm/μs. However, to satisfy the gas requirements specified in section 3, we have, as mentioned earlier, chosen the FMS gas with a drift velocity of ~ 5 cm/μs, resulting in an expected resolution of ~ 250 μm. Pairs of pulses which originate from the same hit are associated by requiring the difference of their arrival times to be less than the full propagation time through the two sense wires of the linking resistor.

The collected charge is found by integrating the digitisings of the pulses from the two wire ends over intervals of the same length, with subtraction of a constant background. A correction for fractional time bins was found to be important since the start times for the two pulses are subject to variable propagation delays. With cosmic muons in the test setup we found a charge-division versus distance characteristics which was linear to about 1%, which is well matched to the resolution.

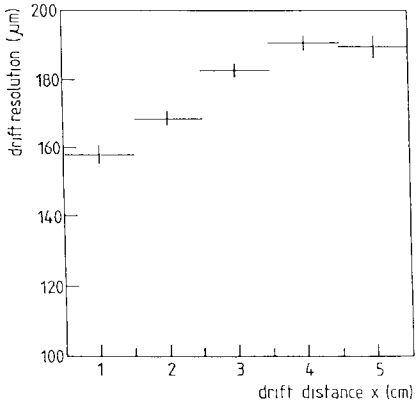

Fig. 4. The space resolution of a drift cell as a function of drift distance for the gas mixture 90% argon and 10% propane (drift velocity 4 cm/μs).

6. Track reconstruction

The space points obtained from the charge–time analysis of the chamber hits are used in a three-step procedure for track reconstruction which starts with the pairing of hits in each double layer followed by association of pairs into straight track segments and finally the linking of track segments through the toroid to form full tracks and thus provide a momentum measurement. Pair finding in the double layers is decisive due to the displacements of cells which results in the sum of drift times being a constant (compare Fig. 1b). A vertex pointing requirement is applied as selection criteria but also unpaired hits are kept to be considered in the track segment finding where we demand three out of four hits in the θ-layers. The measuring errors of the space points for a pair define a cone which is extrapolated to the other θ-layer on the same side of the toroid. In the area defined by the cone, hits are tried for segment fits and are selected by a χ^2-cut. In the future the information from the ϕ-layers will also be used.

For the linking procedure each pretoroid segment is tracked through the magnetic field of the toroid, taking into account energy loss and multiple Coulomb scattering in the magnet iron. By doing this for a minimal reconstructable momentum of 2.5 GeV/c in the spectrometer and for either of the two muon charges possible, regions in the θ-layers after the toroid are defined inside which segment candidates for linking are consid-

ered. From the crossing angle of two linked segments an estimate of the momentum is made. Starting from the pretoroid segment and the estimated momentum the tracking is repeated as the momentum is changed in small steps around the estimated value. Each post-toroid segment obtained from the tracking is compared to the actual segment found and a χ^2 is calculated. The minimum of the χ^2 variation with momentum defines the momentum corresponding to the best fit.

Fig. 5 shows a schematic side view of the H1-detector with the central and forward tracking devices and the calorimeter all surrounded by the instrumented iron. The forward muon spectrometer can be seen to the left of the main H1-detector. A clear muon track originating from the vertex region can be followed through the various subdetectors extending all the way to the end of the forward muon spectrometer. The track coordinates are given by the radial distance from the beam line, R, and the longitudinal Z-coordinate in the direction of the proton beam. However, since the instrumented iron only gives information on the vertical position, X, a radius coordinate cannot be extracted and consequently this track segment is plotted in X, Z-coordinates. This results in the apparent non-alignment of that particular track segment.

7. Drift velocity and T_0 determination

Beam halo muons are used to determine the drift velocity. From the uniform population of the total number of tracks (N) over the full drift distance (ΔY), recorded in a run, a rectangular distribution is expected if the drift velocity is constant. However, due to field variations close to the sense wire, dependence on the angle of the track, the possibility of tracks traversing only the corner of a cell etc., the drift velocity will

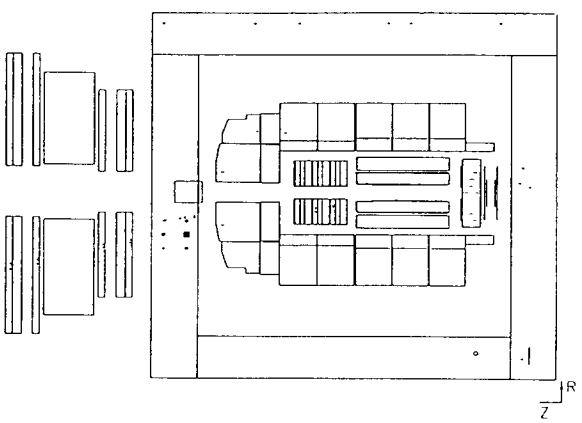

Fig. 5. A side view of a genuine event with a muon penetrating the complete detector.

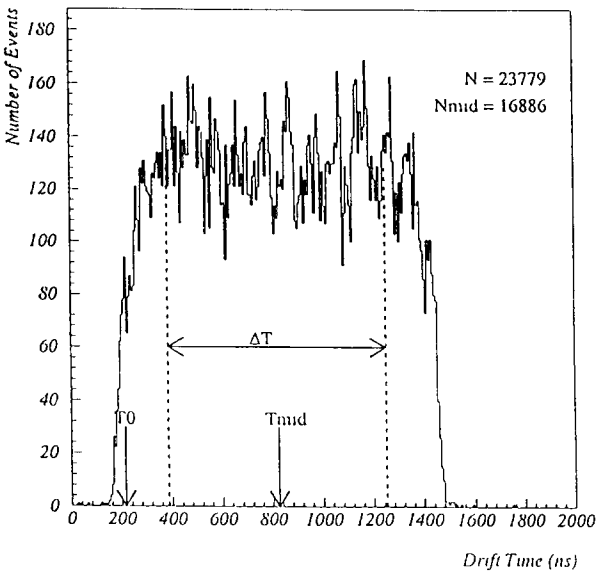

Fig. 6. The drift time distribution for beam halo tracks used to extract T_0 with the FMS-gas

be altered and cause a smearing of the distribution (Fig. 6). In spite of this smearing, the drift time (T_{mid}), corresponding to half the drift distance (3 cm), can be defined as the time which leaves equal number of tracks above and below. Taking an arbitrary time interval (ΔT) symmetrically around T_{mid}, where the distribution is still flat, we can count the number of tracks (N_{mid}) in this interval and use it for a determination of the drift velocity by the following expression:

$$v = \Delta Y N_{\mathrm{mid}}/(\Delta T N).$$

The result is $v = 4.926 \pm 0.039$ cm/μs.

T_0 is determined from the specific geometry of the detector which makes one of the following check sums true for each track.

$$T_1 + T_2 + T_3 + T_4 = 4T_{\mathrm{mid}},$$

$$T_1 + T_2 - T_3 - T_4 = 0,$$

where T_1, T_2, T_3 and T_4 are drift times in the four θ-layers. The first check sum thus will provide an independent measurement of T_{mid}. T_0 can now be determined from the expression:

$$T_0 = (3\ \mathrm{cm}/v) - T_{\mathrm{mid}}.$$

The widths of the two check sum distributions can be used to find the spatial resolution of the chambers.

8. Chamber alignment

The drift chambers must be aligned with respect to each other and to the rest of the detector. The cells of a θ-layer are positioned on its supporting Al-frame to a

precision of ~ 50 μm along the drift direction and to ~ 1 mm in the two other directions. This is better than the achievable resolution and therefore we only have to consider the alignment of the full octants.

Simulation studies and analysis of a small sample of real data have shown that beam halo tracks are suitable for providing the two translational and one rotational quantities which are needed to specify the position of the octant in the plane transverse to the beam direction. Further studies with angle tracks together with the survey will determine the relative positions of the octants along the direction of the beam [5].

Acknowledgements

We wish to acknowledge the substantial effort from the mechanical and electronic workshops at the Universities of Lund and Manchester, together with the contributions of the engineers from the PAG group at the Rutherford Laboratory. We thank the Swedish and United Kingdom funding agencies for their financial support to the construction of the detector. Further we acknowledge the technical facilities provided at the installation phase by DESY.

References

[1] I. Abt et al., DESY Preprint 93–103 (1993).
[2] G. Kessler and W. von Schröder, private communication.
[3] J. Bürger et al., Nucl. Instr. and Meth. A 279 (1989) 217.
[4] R.J. Ellison and D. Mercer, H1 Internal Note 4/87–63.
[5] P. Sutton, Ph.D. Thesis, University of Manchester (1993).